Title: A Field Analysis of New Overhead Line Conductor Coatings to Increase Ampacity/Reduce Power Losses in Desert Environment: Performance and Durability Assessments after 12 Months of Operation

Authors

Dr Oliver Higbee	Ahmad Al-Thagafi	Emam Jalal	Dr Niall Coogan
AssetCool	GCCIA	Midal Cable	AssetCool
United Kingdom	Kingdom of Saudi Arabia	Kingdom of Bahrain	United Kingdom

Key Words: Conductors, Coatings, Ampacity, Power Losses, Solar Reflectivity, Emissivity

Abstract

The peak temperature of overhead power lines limits the capacity of electricity grids. High conductor temperatures increase resistive losses and limit the current carrying capacity of conductors of a given cross sectional area. Exceeding a conductors thermal limit increases sag beyond approved clearances. There is also a risk of loss of strength in aluminium wires when operated outside of specification.

Conductor coatings developed by AssetCool reduce overhead line conductor temperatures by simultaneously reflecting solar radiation and increasing heat dissipation, reducing operating temperature for a specified current. This technology is of particular value in regions with consistently high ambient temperatures and high levels of solar radiation, like GCC and MENA countries.

To verify the performance of coated conductors a field trial was conducted in the Kingdom of Saudi Arabia. The field analysis was conducted in collaboration with the Gulf Cooperation Council Interconnection Authority (GCCIA), at the GCCIA test station in Al Fadhili, KSA. This paper reports over 12 months of data from a field trial testing standard, uncoated ACSR conductors against conductors coated with a proprietary coating developed and patented by AssetCool. High resolution conductor temperature data is presented for standard and coated conductors for the test period. To verify durability, brand new conductors were installed on the rig after 12 months for comparison to field aged conductors. This provides a quantitative comparison of aged and new conductors. Finally, Scanning Electron and Optical Microscopy, Water Contact Angle, self-cleaning, White Light Interferometry, FTIR, current cycling and visual assessments are all also presented.

Peak cooling of up to 33.6% was demonstrated. 12 month field aged conductors and newly installed conductors had a negligible temperature difference. Accordingly, it is concluded, introduction of this new coating to OHTL conductors can improve transmission capacity, reduce power losses, carbon emissions, capital and running cost of transmission lines. It is also concluded they possess suitable durability for long term operation on power lines.

Executive Summary

Problem this Paper Explores: Improving the Thermal Rating of Overhead Conductors

At a macro level, mass electrification and economic growth is driving increases in peak electricity demand and in turn the need for greater transmission and distribution (T+D) capacity. A limiting factor of T+D networks is the thermal rating of overhead conductors. This is especially true in GCC environments, characterised by high ambient temperatures and high solar radiation. Such environmental conditions increase overhead conductor temperatures, in turn limiting the current carrying capacity of overhead (T+D) conductors. In such climates, the Maximum Allowable Conductor Temperature (MACT) is reached with lower current levels compared to other climates.

Conventional, uncoated overhead conductors are not optimised with respect to radiative cooling. They absorb significant amounts of solar radiation (i.e. have a high Solar Absorptivity, α) and do not optimally convert heat energy into radiant energy for dissipation into the atmosphere (sub-optimal Thermal Emissivity, ε). Inefficient heat dissipation coupled with significant solar absorption increases the temperature rise as a function of current transmitted, reaching the MACT at a lower current level.

Solution: Spectrally Selective Coatings to improve Conductor Performance

Engineering the surface of overhead conductors to minimise solar absorption (via high solar reflectivity) and maximise heat dissipation. This occurs via a "spectrally selective" coating (SSC) which operates independently in two regions of the EM spectrum (solar spectrum and IR spectrum).

Research

A field trial rig was constructed at the Gulf Cooperation Council Interconnection Authority (GCCIA) test station, Al Fadhili, KSA. Conductors of the same specification were tested. Control conductors were used as received. Test conductors were coated with a SSC formulated specifically for application to overhead T+D conductors.

High resolution field data over a 12 month period was collected and presented. At the 12 month stage a brand new coated conductor "SSC-New" was installed on the rig for comparison to the 12 month exposed conductor "SSC-Aged" to quantitively analyse variations in cooling performance after 12 months exposure. Additional laboratory data is also presented.

Results

- Peak cooling of up to 33.6% was demonstrated. An average monthly temperature difference of ~6.3% was demonstrated for 12 months.
- The substantial difference between the peak cooling and the average cooling was due to the consistently high wind speeds (average ~4 m/s across the year) at the Al Fadhili site, intentionally chosen for its harsh durability challenges (sand erosion).
- SSC-New and SSC-Aged conductors exhibited no measurable thermal performance difference (Δ~0.1°C).
- Scanning Electron Microscopy confirms no reduction in film thickness after 12 months and Fourier Transform Infrared Spectroscopy confirms no change in chemical bond structure after 12 months.
- Laboratory test results showed improved SSC hydrophilicity after 12 months.

Introduction

Total electrical energy consumption in the GCC countries is forecasted to reach 2000 TWh by 2040, from 800 TWh in 2020 [1]. Relatedly, there is a need to increase the capacity of the T+D infrastructure. Via an extended field trial and laboratory analysis, this paper explores "Spectrally Selective Coatings" (SSCs) as an innovation to increase the capacity of overhead T+D conductors.

Previous research papers extensively outline the theory behind SSC's and their ability to improve conductor performance [2]. Briefly, using CIGRE 601 models, it can be seen that by minimising solar absorption and increasing thermal emissivity, capacity increases of up to 30% can be delivered in environments where the ambient temperature is 50°C [3]. Via dynamic CIGRE 601 modelling and statistical comparison to empirical field data, Ref [2] confirms that a proprietary SSC can offer such performance data in GCC conditions.

However, following [2] several core research questions remained. T+D conductors are long term infrastructure with decades of operation. Research needs to demonstrate the long term performance of the coating and if there are any variations in cooling performance over time. In addition to this, laboratory analysis needs to confirm if there has been environmental degradation of the coating material after exposure in the harsh GCC conditions. Other areas of interest include the potential impact/composition of pollutants on the performance and properties of the coating. Data is provided to answer these questions.

Specifically the following is presented: coating thickness and surface composition analysis by Scanning Electron Microscopy (SEM). Visual assessments of water contact angle, self-cleaning and cleanability. White Light Interferometry (WLI) analysis of surface roughness. Fourier Transform Infrared (FTIR) spectroscopy is used to investigate if any changes to chemical bonds occurred, due to degradation. Coating defects were analysed by optical microscopy. Finally, thermal cycling stability is tested by conductor current cycling in accordance with ANSI C119 [4].

This paper is organised as follows: firstly, we outline the methodology used for experimentation which is comprised of the field trial experimental design and post-trial analysis and the results from this. Following this we discuss the laboratory and field trial results before making conclusions on material performance and durability. Finally, we conclude with our future research plans.

Methodology

Building on the previous paper [2] this section outlines the methodology for the field trial performance after 12 months and the methods for analysing the condition of the conductors and the comparison to a newly applied coating both in the field and in a laboratory.

Field Analysis of Performance

Please see [2] for extensive details on field trial and experimental design, which is consistent with other published experiments of this nature [5]. Briefly, a purpose-built field trial rig was constructed at the GCCIA Test Station in Al Fadhili, Kingdom of Saudi Arabia. Six 7.5 m Quail ACSR/AS conductors were sourced. Three were coated with a proprietary SSC. Three were installed as received. All conductors were connected electrically in series and DC power was supplied. T-type thermocouples were inserted into the conductor cores (8 per line), and these were connected into a National Instruments CompactDAQ Chassis (cDAQ-9178) via conditioned modules (3xNI-9213 Spring Terminal TC modules). Further, a dedicated weather station (ClimaVUE50) was installed on site to capture high resolution weather data, including air temperature, wind speed, wind direction and solar radiation.

In summary, six conductors (3 x coated (test) and 3 x uncoated (control)) of the same specification were spatially collocated with the same orientation to the sun/wind and hence had the same environmental exposure. They were connected electrically in series and had the same current. High resolution thermal and weather data was collected to determine the effect of the coating in field environments. The initial 12 month field trial was completed and data will continue to be collected. Results for the first 12 months (April 2021 – March 2022) are illustrated and analysed below.

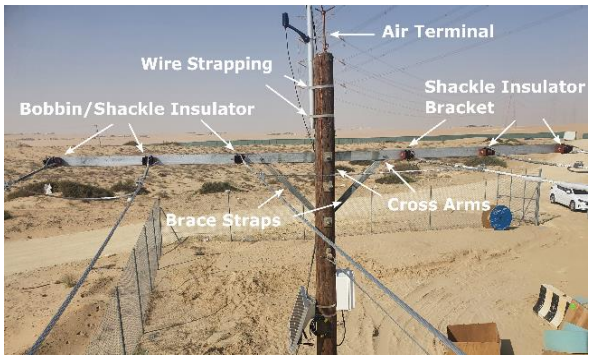

Figure 1: Field trial cross arm set up.

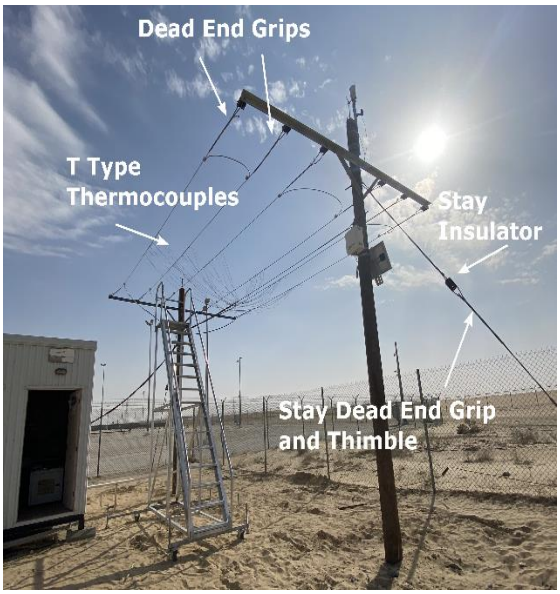

Figure 2: Field trial testing span constructed at GCCIA Test Station in Al Fadhili, Kingdom of Saudi Arabia.

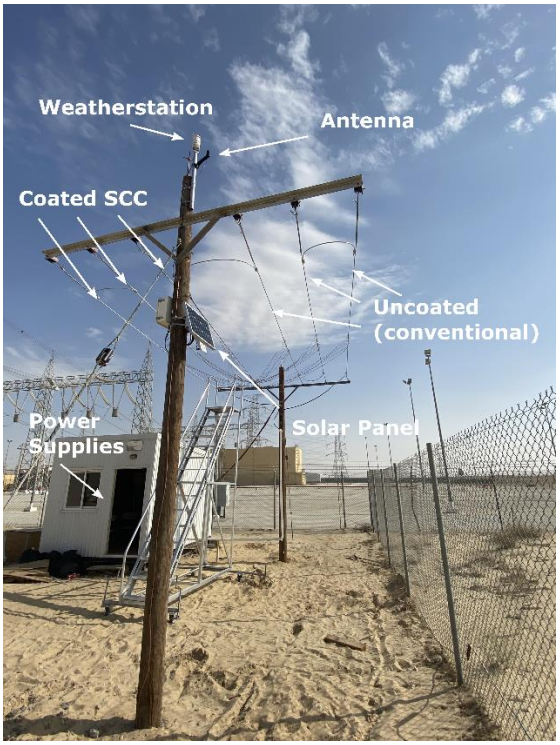

Figure 3: Field trial testing span constructed at GCCIA Test Station in Al Fadhili, Kingdom of Saudi Arabia.

Field comparison of new and aged coated conductors

Post Exposure Laboratory Analysis
After completing the 12 month field trial of continuous thermal load on the conductors at Al Fadhili, one of the three coated conductor spans was removed from the field trial rig. This provides a conductor sample with 12 months field exposure "SSC-Aged". This conductor was then tested in the laboratory to understand it's condition and contrast that with a newly produced conductor "SSC-New" and an "SSC-unexposed" conductor which had been produced in the same batch as the SSC-Aged samples but had not been tested under load or exposed to the environment. The laboratory analysis is summarised in the following section.

Performance Consistency: Aged vs New
In the vacant span on the field trail rig, a "SSC-New" sample was installed. This provides a controlled analysis of aged vs new conductors in field environments. The conductors were then energised back to 370A DC and the temperatures were collected, using the same methodology as coated vs uncoated. After 30 days the thermal performance of the newly installed coated conductor was analysed and compared against the two-remaining SSC-aged conductors. Analysis was broken down into periods of days, weeks and a month to reveal any differences in thermal performance with aging.

Laboratory testing SSC-New and SSC-Aged
In the previous paper [2] newly coated samples were subjected to a selection of tests to artificially age them and determine the coating's durability on an asset with a long-life cycle. This included: UV stability, corrosion stability, temperature stability, chemical stability, moisture stability, humidity stability and sulphur dioxide resistance. Results can be found in the previous paper [2].

Building on this body of work, a series of tests were carried out on the coated conductor span removed from the rig to determine the effect of the harsh environment on the coating and on the conductor after 12 months of continuous load. These are described below.

<u>SEM Analysis: Layer thickness, film integrity and pollutant analysis</u>
Scanning electron microscopy analysis of "SSC-New" and "SSC-Aged" was completed. Measurements of the surface texture, composition of surface contaminants and coating thickness were carried out. This was to determine if coating had been eroded or damaged in the field and what contaminants the coating was not able to clean from it's surface.

Samples for coating thickness were mounted in resin blocks and polished. Due to the dielectric nature of the coating, a film of carbon (nominally 10 nm) was evaporated onto the surface prior to

analysis, to prevent charge build up and allow for clear imaging. Two cross sectional samples of each conductor were taken and images of the "SSC-Aged" and "SSC-New" samples were captured to reveal surface texture and coating thickness. The compositional analysis returned the elements present. The presence and sources of these elements and their likely compounds were then investigated.

Current cycling

The thermal and electrical stability was analysed in a laboratory environment. 1m sections of SSC-new and SSC-aged were current cycled in accordance with ANSI.C119 [4]. The wind, light, humidity and ambient temperature were controlled. The SSC-New and SSC-Aged samples were electrically connected in series to ensure they experience the same current and K-type thermocouples were inserted into the conductor cores (4 per sample). The conductor temperatures were collected at one second intervals via two Pico Technology TC-08 data loggers using PicoLog 6 software. The ambient temperature was also collected via a K-type thermocouple connected to the Pico Technology data logger.

The experiment consisted of 100 cycles, each one hour in duration. For the 'on' cycle, 290A DC was applied to the conductors via three 1500w direct current, remotely programmable (DC) power supplies (Kikusui PWX1500L), 290A was chosen to ensure the ACSR's maximum allowance conductor temperature (MACT) was reached on each cycle. The 'off' cycle, also one hour in duration, consisted of no load applied to the conductors, to allow cooling to room temperature.

Surface roughness

Surface roughness is an important parameter in determining the amount of corona loss and noise a conductor produces under the high electromagnetic fields typically encountered on transmission lines. 0.2m samples of SSC-new and SSC-aged were analysed with a White Light Interferometer (WLI)). Analysis was conducted with a Bruker Contour at two magnifications: 20x (an area of 0.24 x 0.35mm) and 50x (95 x 125 µm area). The roughness variation with high magnification is not uniform. Microstructures affect the roughness measurement at lower magnifications which become more defined with higher magnifications. For each sample a minimum of three measurements were conducted on different areas of the sample with results presented as an average of those measurements.

Water Contact Angle

The hydrophobicity of a coating can be defined by measuring the angle water droplets form on its surface. Hydrophobicity can play a key role in cleaning pollutants off the surface during periods of rainfall. SSC-aged and SSC-new conductor samples were placed on an even surface, and 5µL of deionised water was applied to the uppermost surface using a micropipette (Four E's Scientific Micropipette, 10 µL tip size). Images of the static droplet were captured at a distance of 15 cm and qualitatively analysed.

Microscopy

Microscopy was performed using a Yenway SZN71 stereo microscope, fitted with LED-60T 4W illuminator, at 4.5X magnification. Images were taken using the mounted YenCAM 3500 (5 MP) and the operating software YanCam Version 5.0.

Self-Cleaning

The SSC-aged and SSC-new conductors were tested for self-cleaning ability. A resazurin (Rz)-based photocatalytic indicator dye was prepared as described in the literature [6]. Due to the unconventional geometry of the conductors, the dye was applied with a paintbrush (instead of a calibrated wound bar applicator) and compared to an equivalent sample applied on a flat panel, to give an estimated film thickness of approx. 0.9 µm. The dye-coated conductor was placed in an oven at 70 °C for 10 minutes to dry and upon removal was placed in a sealed box and irradiated with UV light (30 mW cm^{-2}, discrete bulbs: 275 nm, 365 nm, 395 nm) and the reduction of the Rz monitored *via* the colour change from blue to pink.

FTIR Spectroscopy

FTIR irradiates samples with IR radiation. The chemical bonds absorb IR at characteristic wavelengths and can be compared to a known library. FTIR analysis can provide data on if key bonds have undergone change or chemical depredation. The Infrared spectra of an SSC-unexposed and an SSC-aged conductor sample were measured using a Bruker Alpha II spectrometer fitted with the platinum ATR module. The 400 to 4000 cm-1 region of the IR spectrum was analysed.

Results

Weather statistics

Al Fadhili test station represents a harsh environment for overhead lines. Situated within 30km of the Arabian Gulf and on the outskirts of the Industrial city of Al Jubail, conductors are exposed to high humidity, salinity and pollutants. This combined with the climate: a desert environment, exposed to high summer temperatures, little rain and high wind speeds, can greatly reduce the lifetime of many overhead line assets. Al Fadhili test station was chosen specifically due to these testing conditions.

Monthly average wind speeds of 3.0 m/s – 5.7 m/s have been recorded by the weather station as shown in Table 1. These high wind speeds combined with the desert sand regularly induces sand-based erosion, hence the coating material being tested here.

Table 1: Monthly Averages.

	Amb* (°C)	Wind Speed (m/s)	SR (W/m^2)	RH (%)
Apr 21	28.0	4.0	207.7	30.9
May 21	34.0	3.2	234.5	22.4
Jun 21	36.4	5.7	203.7	20.2
Jul 21	38.0	3.3	220.9	31.3
Aug 21	37.1	3.0	198.9	34.2
Sep 21	33.1	3.8	172.3	38.3
Oct 21	28.6	3.1	138.5	53.3
Nov 21	22.6	3.6	111.1	57.2
Dec 21	17.4	4.2	116.3	60.1
Jan 22	15.0	4.4	135.2	69.5
Feb 22	17.5	4.5	172.9	58.0
Mar 22	20.8	4.9	205.0	46.1

**Amb – ambient temperature, SR – solar radiation, RH – relative humidity.*

The data shows wind speeds were correlated to solar radiation intensity, whereby the highest average wind speeds were recorded during the periods of most intense sunlight. This can be seen by separating those recordings by day and night, as shown in tables 2 and 3. It is visible that consistently high wind speeds are recorded during the day (3.9 m/s – 7.2 m/s) on average.

Table 2: Monthly Daylight Weather.

	Amb* (°C)	Wind Speed (m/s)	SR (W/m^2)	RH (%)
Apr 21	30.7	5.0	376.9	24.9
May 21	36.9	4.1	404.4	17.5
Jun 21	38.9	7.2	349.6	17.1
Jul 21	40.6	4.3	381.1	25.4
Aug 21	40.0	3.9	359.6	26.8
Sep 21	36.1	5.1	323.8	29.8
Oct 21	31.6	4.3	277.8	42.7
Nov 21	25.3	4.7	236.3	47.1
Dec 21	19.5	5.2	253.7	53.2
Jan 22	16.6	5.2	289.8	63.1
Feb 22	20.2	5.9	352.7	47.3
Mar 22	23.3	5.8	393.9	38.9

Table 3: Monthly Night-time Weather.

	Amb* (°C)	Wind Speed (m/s)	SR (W/m^2)	RH (%)
Apr 21	24.6	2.9	0.0	38.3
May 21	30.1	2.0	0.0	29.2
Jun 21	33.1	3.6	0.0	24.6
Jul 21	34.4	1.9	0.0	39.5
Aug 21	33.5	1.9	0.0	43.4
Sep 21	30.4	2.3	0.0	47.7
Oct 21	29.7	2.3	0.0	47.9
Nov 21	25.7	2.0	0.0	63.7
Dec 21	20.3	2.5	0.0	66.2
Jan 22	15.6	3.3	0.0	66.0
Feb 22	13.6	3.7	0.0	75.1
Mar 22	14.9	3.1	0.0	68.2

Table 4 shows the large range in weather conditions seen at Al Fadhili, with temperatures starting at 4.5°C and peaking at 49.7°C. High wind speeds up to 19.9 m/s have been recorded and the relative humidity has varied between 5% and 100% (rain). Solar radiation up to 951 W/m^2 was also seen. These ranges underline the harsh conditions the conductors have encountered.

While the high wind speeds are important for testing the coating's durability, they also have a large effect on the cooling as seen in this region. To demonstrate this, the heating power of solar radiation on a conductor is calculated [3]. This is then directly compared with the conductor cooling power generated by wind [3].

The solar heating and convection cooling are directly compared in Figure 12, illustrating that convection loss is dominant. This dominance results in higher conductor temperatures when

wind speeds are low regardless of solar intensity. Table 2 and 3 show significantly lower wind speeds at night therefore conductor temperatures are expected to be higher during this time. As convective cooling generally dropped during the night it can be forecasted that the coating will have a larger impact on the conductor temperature because radiative cooling power becomes more central to the heat balance equation as the contribution of convective cooling decreases [3].

Table 4: Minimum and Maximum Weather readings recorded (averaged over one minute).

	Amb* (°C)		WS*	SR*	RH (%)	
	Min	Max	Max	Max	Min	Max
Apr 21	14.3	42.6	18.8	925	6.5	96.8
May 21	21.4	48.5	12.5	950	5.3	76.8
Jun 21	26.3	49.1	19.9	800	6.2	62.6
Jul 21	26.0	49.5	11.8	874	6.8	100
Aug 21	26.5	49.7	11.7	729	7.8	85.5
Sep 21	23.5	47.4	14	668	8.7	94.3
Oct 21	18	42.8	13.4	591	11.1	100
Nov 21	12.6	36.3	11.4	560	18	100
Dec 21	6.5	29.6	14.5	814	19.2	100
Jan 22	4.5	27.6	14.9	819	20.4	100
Feb 22	8.3	33.1	15.1	810	17.4	100
Mar 22	5.8	39.8	17.5	951	8.8	100

**WS – Wind speed (m/s), SR – solar radiation* (W/m^2), *RH – relative humidity.*

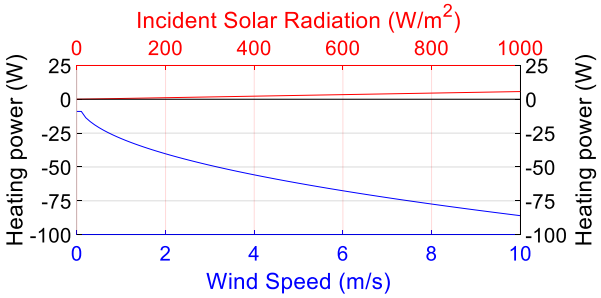

Figure 4: Heating power of solar gain compared to cooling power of convection.

Conversely at higher wind speeds, convective cooling dominates the heat balance equation, resulting in a smaller average temperature difference between coated and uncoated conductors [3]. This is illustrated in Figure 5, where the temperature difference between coated and uncoated conductors exponentially decreases as the wind speed increases from 0.5 m/s to 10 m/s. The largest rate of change is found from 0.5 m/s to 5 m/s where the temperature difference decreases from over 20°C to 5.5°C. The temperature difference falls below 3°C at 10 m/s. Whilst this lowers the average temperature difference over windy periods, it does not limit the value of the SSC as it can be difficult to accurately forecast periods of low wind, spatially (along the conductor) and temporally. An error in rating with respect to low winds can cause thermal aging and conductor failure [7].

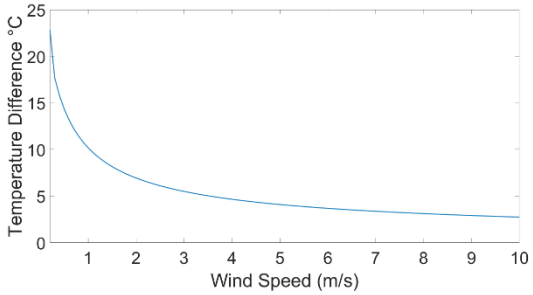

Figure 5: Temperature difference between SSC Conductor and Conventional ACSR as a function of wind speed, as calculated by CIGRE-601 [3]. Model Parameters: Quail ACSR/AS, wind direction 45° to the conductor axis, 500 W/m^2 Solar Radiation, 40°C Ambient Temperature, 380A DC current.

SSC Cooling Data

This section outlines the conductor temperature and cooling data recorded. Both monthly averages and peak cooling data are presented. Due to the consistently high wind speeds, the lines are regularly cooled by convection. Table 5 highlights that the average cooling over the monthly periods was 2.50 – 9.49%. The data for the month of February was missing due to a data collection hardware failure, the hardware was replaced and data collection restarted in the first week in March 2022.

Table 5: Average monthly conductor temperatures.

	Conventional	SSC	Cooling (%)
Apr 21	64.92	59.55	8.27
May 21	65.11	60.49	7.11
Jun 21	57.57	56.13	2.50
Jul 21	67.35	64.13	4.79
Aug 21	67.72	64.04	5.43
Sep 21	61.27	57.86	5.57
Oct 21	60.67	55.99	7.71
Nov 21	58.18	52.66	9.49
Dec 21	63.49	58.19	8.34
Jan 22	57.17	52.95	7.39
Feb 22	-	-	-
Mar 22	54.54	52.84	2.94

As shown in Tables 2 and 3, higher wind speeds were found during the day, which should result in less cooling during the day and more effective radiative cooling at night. Table 6 and 7 split the monthly trends into day and night periods with the average cooling being much higher at night (3.77-12.58%), due to the lower wind speeds experienced at night resulting in reduced convective cooling and increasing dominance of radiative cooling [3].

Table 6: Average monthly Daytime conductor temperatures.

	Conventional	SSC	Cooling (%)
Apr 21	63.19	59.15	6.39
May 21	62.66	59.70	4.73
Jun 21	53.67	53.58	0.16
Jul 21	64.93	62.91	3.10
Aug 21	65.28	63.22	3.16
Sep 21	57.77	56.34	2.46
Oct 21	56.52	53.70	4.98
Nov 21	54.14	51.04	5.72
Dec 21	50.69	47.65	6.00
Jan 22	51.88	49.80	4.01
Feb 22	-	-	-
Mar 22	51.60	50.91	1.33

Table 7: Average monthly Night-time conductor temperatures.

	Conventional	SSC	Cooling (%)
Apr 21	66.97	60.01	10.38
May 21	68.37	61.53	10.04
Jun 21	63.13	59.76	5.33
Jul 21	70.59	65.75	6.86
Aug 21	70.76	65.08	8.03
Sep 21	65.06	59.49	8.55
Oct 21	64.66	58.20	9.99
Nov 21	63.30	55.34	12.58
Dec 21	59.74	53.17	11.00
Jan 22	58.25	53.24	8.59
Feb 22	-	-	-
Mar 22	54.79	52.72	3.77

An example cooling day is demonstrated in Figure 6. The blue line denotes the average of the 3 lengths of Quail ACSR/AS with a spectrally selective coating (SSC) applied. The grey line is the average of the 3 conventional Quail ACSR/AS spans and yellow the ambient air temperature. As seen, the SSC lines remained consistently below the conventional lines, with the largest differences seen when the temperature peaks in periods of low wind. These spikes are critical periods to cool. Here we ran the spans at 380A, far above the recommended thermal rating. The conventional conductor regularly exceeded the MACT whereas the SSC remained below this crucial threshold.

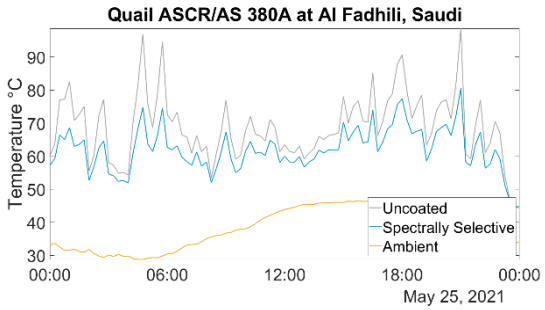

Figure 6: Coated and uncoated Quail ASCR/AS conductor temperatures in Al Fadhili, Saudi at 380A DC. Ambient Air temperature shown in gold. Average Metrological data. Wind Speed =2.7 m/s, Direction = 0° Solar Radiation =216 W/m².

By focusing on periods where convective cooling is low, the effect of the SSC can be seen. Figure 7 shows a 4 hour period during the day with wind speeds between 1.3 m/s and 2.2 m/s. Here the lower solar gain and higher radiative cooling afforded to the SSC lines are more visible.

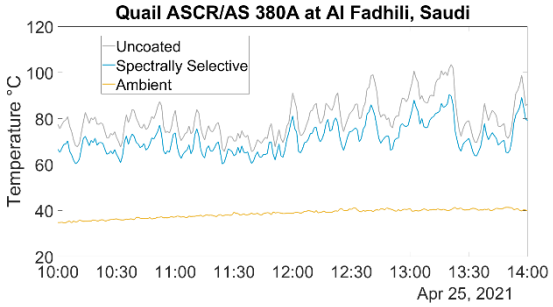

Figure 7: Coated and uncoated Quail ASCR/AS conductor temperatures in Al Fadhili, Saudi at 380A DC. Ambient Air temperature shown in gold. Average Metrological data. Wind Speed =1.75 m/s, Direction = 30° Solar Radiation =670 W/m².

Peak cooling outlines the temperature reduction in "worst case scenario conditions" to which conductors are regularly rated. *e.g.* low wind, high solar radiation and high ambient temperatures. The peak cooling periods for each month is shown in Table 8. Peak cooling temperatures of 16.9% - 33.6% have been demonstrated. It should be noted these peaks were recorded in weather conditions far from the worst-case scenario conditions

outlined in the summer scenarios (1.1-2.1 m/s wind, 0 W/m solar, 23.6-33.6°C ambient).

Table 8: Peak cooling periods in each month.

Time Stamp	Bare	SSC	Cooling
28 April 21 04:37	103.5	78.9	23.7%
04 May 21 22:34	105.3	76.5	27.4%
09 June 21 21:26	100.1	78.9	21.2%
30 July 21 04:31	88.0	71.2	19.1%
31 August 21 07:27	100.8	67.2	33.6%
02 September 21 06:01	79.6	57.3	28.0%
28 October 21 07:31	105.9	78.3	26.10%
18 November 21 20:59	91.7	65.8	28.20%
07 December 21 20:52	103.2	70.6	31.60%
23 January 22 21:35	103	75.6	26.60%
February	-	-	-
30 March 22 03:45	88.8	73.7	16.9%

Table 8 also illustrates a key phenomenon of the SSC. The conventional conductor has clearly exceeded the MACT and the capacity of the network would have to decrease until the conductor temperature is below MACT. However, with an SSC, the current on the test span did not have to be decreased and capacity would not be affected. It can be seen that without the SSC exceeding MACT (80°C), the cooling performance has been measured up to 33.6%. The non-exceedance of MACT by the SSC is seen consistency throughout the 12months of the trial. The variation of peak cooling each month is directly proportional to the weather conditions encountered. With the combination of lowest stable wind speed and humidity occurring in August (33.6%).

Another key advantage of the SSC is power savings, using the differences in resistance caused by the difference in operating temperatures between the conductors, power savings (I^2R) were calculated on peak cooling days and extrapolated out to a kilometre span as shown in Table 9. The data shows no loss of peak cooling and power loss savings in the first 10months of the trial, with the highest power savings (2.7%) found in month 7 and 9. The drop in performance in month 12 can be explained by non-ideal peak cooling conditions and the performance of a 12month old conductor is discussed in the next section. It should be noted, that as the environmental conditions limit the current carrying capacity of conductors the power losses are relatively low (1-3%). However, in higher capacity conductors where current levels are higher, power loss reductions of 5-10% are achievable.

Table 9: Power loss savings calculated from lower operating temperature.

Time Stamp	Bare	SSC	Cooling	Power savings per km (kWh)	% Power Loss Savings
23 April 21	74.0	65.9	10.9%	45.2	2.6
24 May 21	78.8	70.7	10.3%	45.6	2.5
01 June 21	64.1	60.9	5.1%	18.5	1.0
22 July 21	76.2	69.8	8.5%	36.3	2.1
18 August 21	71.9	66.5	7.6%	30.7	1.8
09 Sept 21	77.9	70.4	9.7%	42.5	2.5
27 Oct 21	73.2	65.1	11.10%	43.2	2.7
02 Nov 21	69.2	61.7	10.90%	40.1	2.5
07 Dec 21	62.6	54.7	12.50%	41.9	2.7
17 Jan 22	71.9	64.4	10.40%	40.1	2.5
Feb	-	-	-	-	-
31 March 22	61.9	59.1	4.6%	15.2	0.98

Benchmarking

Table 10 shows the average temperatures of the SSC-New and SSC-Aged conductors for the first month after reconductoring. The temperature difference averaged 0.1°C in the first month, with

a maximum weekly difference of 0.9°C. This is within the experimental error of the thermocouples (±1°C) and it can be concluded that no measurable thermal performance drop off of SSCs took place after 12 months in a harsh desert environment. From analysing the data, we see no increase in temperature was observed during the daylight hours. This shows there has been a minimal drop in solar reflectance. Laboratory testing is presented below.

Table 10: Comparison of a new and 12 month aged SSC. For comparison the uncoated Quail ACSR/SW averaged 54.6°C for the month.

	SSC-Aged	SSC-New	Cooling
Week 1	49.6	48.9	1.4%
Week 2	54.5	54.6	-0.3%
Week 3	53.0	53.9	-1.8%
Month 1	52.8	52.9	-0.3%

Visual Analysis

The laboratory analysis began with a visual assessment of the SSC-aged conductor. Figure 8 shows the SSC-aged conductor. The SSC-aged sample shows no damage to the coating, but there is a visible change in colour. The colour is consistent with a fine sand dust. Table 10 shows how this colour change has been shown to have no impact on thermal performance. A number of hypotheses can be provided here, as off-white colours have lower reflectance in the visible spectrum when compared to bright whites. A leading hypothesis for the consistent performance is that any minor decreases in solar reflectance are compensated for in increased surface roughness further improving emissivity, as there is more surface area to cool over, however further research is required on this point.

Figure 1: Visual assessment of SSC-aged conductor sample

Cleanability

The SSC-aged conductor sample was rinsed under a steady stream of water (tap) for one minute and the visual impact analysed. Figure 9 shows marked improvement in visual appearance, with the cleaned conductor appearing a lot whiter and close to the colour of a newly coated conductor. This shows in desert environments the conductor can be easily cleaned by spraying water in a similar method to insulators [8]. This also demonstrates the significant majority of surface contaminants are settled on the surface and not integrated into the film, further limiting impact on performance or durability.

Figure 2:Visual comparison of SSC-aged before cleaning (left), after cleaning (middle) compared SSC-new (right)

SEM Analysis

Table 11 shows the average thickness of SSC-unexposed and SSC-aged samples. The average SSC-unexposed sample was 17.1 µm and the SSC-aged was 18.4 µm. Small variations in applied coating thickness from application have resulted in the SSC-aged sample having a higher film thickness, however these relative values indicate that no significant erosion in harsh desert environments has occurred. A cross section analysis is shown in Figure 10.[1]

[1] An accurate non-destructive thickness measurement is difficult and was not done before the sample was installed in Al Fadhili, so no conclusion on absolute loss of thickness can be made. There is also potential error here due to natural variations in application as these are difficult to control at micron level. Yet, it is considered a valid data point which shows there has not been substantial erosion of the film thickness.

Table 1: Summary of coating thickness measurements

	SSC-unexposed	SSC-aged
Average coating thickness	17.1 µm	18.4 µm
Standard deviation	4.1 µm	11.1 µm
Number of measurements	20	25

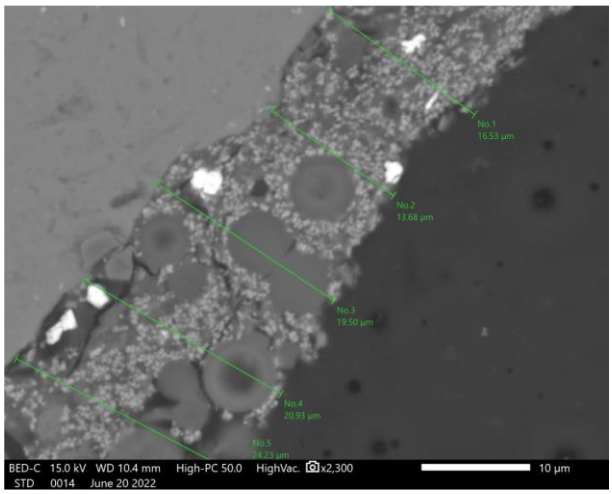

Figure 10: Thickness measurements of a cross section of the SSC-aged. Captured with an JEOL JSM IT510 LV-SEM, using a Secondary Electron Detector (SED) and Backscatter Electron Detector (BED-C). Acceleration voltage of 15kV and working distance of 10mm. Images resolution 1024 and dwell time 26us.

The results of the surface composition analysis showed a significant and consistent calcium and sulphur presence on the SSC-aged surface. The surface contained 14% and 10% (by weight) of calcium and sulphur respectively, compared to no presence of these elements on the SSC-unexposed sample. This indicates a high surface level contamination of $CaSO_4$ on the surface of the exposed coating. The origin of this contamination is deposition of sand on the surface of the coating; it is known that the sand and soil in the eastern regions of Saudi Arabia have a high calcium sulfate (gypsum) content [9][10].[1,2] There is also the presence of aluminium oxide in the same sands, which is plausible given the measured present of aluminium on the surface of the conductor.

Calcium sulfate is also a by-product of many chemical industrial processes, such as flue gas desulfurisation (*via* calcium sulfite) and may have deposited on the coating of the surface through this route, or have formed from the reaction of pollutants $CaCO_3$ and SO_2 in the atmosphere [11][12].

The exposed conductor also shows consistent low levels of iron contamination (1%). This may also arise from iron oxides in the deposited sand and/or pollution from the local area [13]. Not constant across the surface of the whole film, but detectable in two measurements is the presence of fluorine, detected at 10% and 6% at two sites. This is likely from anthropogenic sources such as petrochemicals emissions from the industrial area of Jubail [14]. These are the contaminants that were not washed or self-cleaned off the SSC surface and the effect of their presence on performance will be outlined further down.

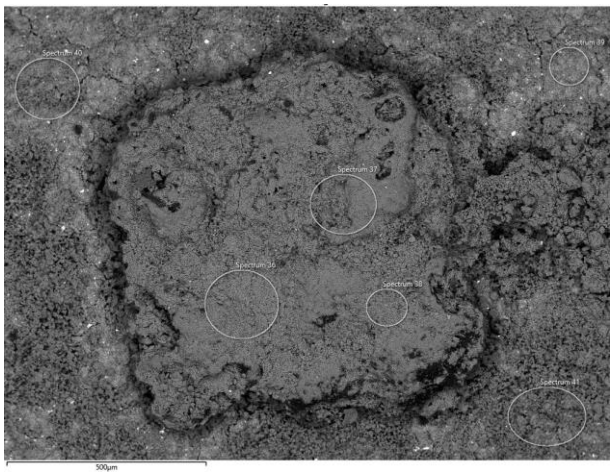

Figure 3: Composition Analysis of the exposed SSC, the white circles indicate the areas analysed.

Unfortunately, the electron beam breaks down organic contaminants that were present in the air or on the sample surface and forms a thin carbon film on the surface, which skews the carbon measurements, this makes further discovery of petrochemical and other organic contaminants impossible with this method. However, this is possible with X-ray photoelectron spectroscopy (XPS) or secondary ion mass spectrometry (SIMS) and will be carried out in the future.

<u>Infrared</u>

Analysis of the FTIR(ATR) spectra of the SSC-new and SSC-aged conductors showed minimal variation between samples, as shown in Figure 12. The spectra were dominated by stretches associated with silica, showing the Si-O-Si symmetric stretch (796/795 cm^{-1}), Si-O-Si asymmetric stretch (1075/1078 cm^{-1}), as well as

peaks which are associated with network pores (1153sh, 1176 cm^{-1}).

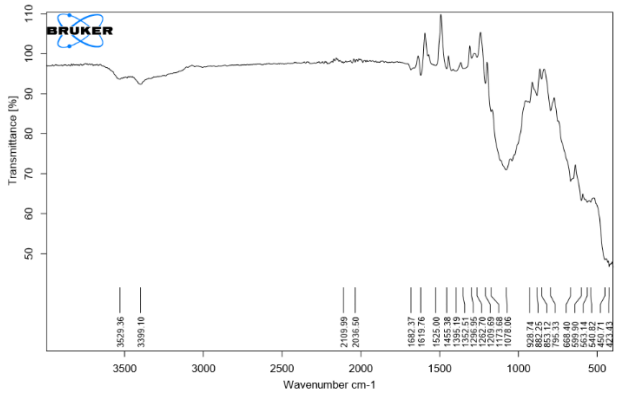

Figure 4: FTIR spectrum of SSC-aged sample

The main difference in the spectra is the observation of broad peaks at 3399 and 3531 cm^{-1} for the exposed conductor. These arise from the presence of O-H bonds in the sample, thought to be present in the Sand [$CaSO_4$ ($CaSO_4.2H_2O$)] identified through the SEM compositional analysis. Table 12 describes the identifiable peaks.

Critically, the SSC material is inorganic in composition where the Si-O-Si chemical bond provides the core properties and durability. As can be seen from Table 12 this core bond remains unchanged and we can conclude there has been no chemical bond scission during the field trial.

Table 2: FTIR identifiable peaks of SSC-aged and SSC-unexposed conductor samples.

SSC-Unexposed	SSC-aged	Identity
796	795	Si-O-Si symmetric stretch
1075	1078	Si-O-Si asymmetric stretch
1153	-	Network pores
1176	1176	Network pores
-	3399	O-H stretch
-	3531	

Current cycling

The results of 100 on/off cycles at 290A, are summarised in Table 13. The difference in the mean peak temperature reached was 0.9°C, this was within experimental error (1°C). Small fluctuations were observed, due to activity in the laboratory environment, and no decline or improvement in performance was observed during the experiment.

Table 13: Current cycling peak temperatures

Sample	SSC-aged	SSC-new
Mean peak temperature	77.8	76.9
Max peak	80.9	79.6
Min peak	76.5	74.9

Surface roughness

The average surface roughness of the SSC-aged conductor was measured to be 7.73 µm compared to 4.42 µm of the SSC-unexposed conductor. This is significant increase is likely caused by the surface pollutants and could negatively influence corona losses if the same pattern emerges under HV loads [15]. Figure 13 shows the surface roughness of an exposed SSC conductor at x20 objective.

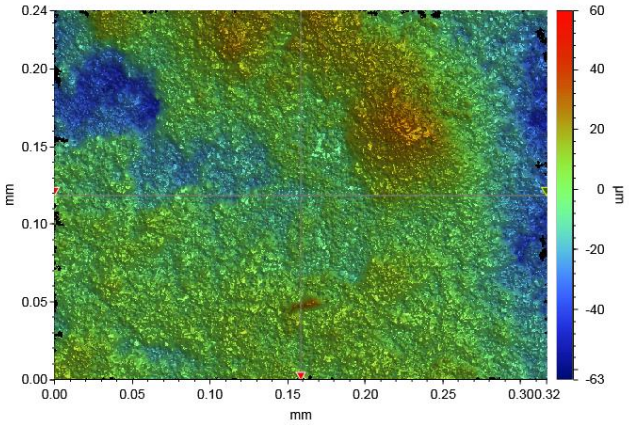

Figure 13: White light interferometer (WLI) surface roughness of exposed SSC conductor. x20 objective.

Water Contact Angle

The SSC was super hydrophobic before installation, this can be seen in Figure 14 where water incident onto the surface, beads. This design choice was to aid the cleaning during rainfall. No water contact angle data could be taken due to the complex geometry of the conductor however there are large observable differences between the samples. The SSC-exposed conductor exhibits high hydrophilicity, characterised by water not forming a bead on the surface. While this would reduce the effectiveness of rainfall cleaning of the coating's surface, it does have a positive effect for corona loss. Corona losses increase on wet conductors. This loss is exaggerated if the conductor's surface is hydrophobic, as the electromagnetic field interacts with the water beads, increasing the loss [16].

Figure 5: Water contact angle test. Water droplet incident on SSC surface. Top: Unexposed conductor Bottom: Exposed conductor.

Microscopy

Microscope images of the SSC-aged and SSC-new are show in Figure 15. The SSC-aged conductor showed a uniform white coating with a light brown/dark yellow, inconsistent surface contamination. This was thought to be primarily sand-based as analysed in the SEM. No cracking or other physical degradation of the coating was observed.

Figure 6: SSC-aged and SSC-unexposed at 4.5X magnification

Self-Cleaning

The redox reaction for the SSC-unexposed conductor under UV exposure occurred after 15 minutes. By contrast the redox reaction occurred within 15 seconds on the SSC-aged conductor, turning blue to pink. This was repeated under ambient light exposure and the reaction occurred immediately again. This suggests an improvement in the self-cleaning however there may be other factors causing this result. The significant increase in hydrophilicity certainly enhances the interface between the dye and the coating's surface resulting in thinner dye layers and more light penetration. This could also indicate the presence of another redox-active species reducing the dye.

Future Work

This field trial will continue into a second year and seek to report on the following: continued side by side performance comparisons of the newly SSC coated conductors compared to those that have been in the field since the start of the field trial. Performance of SSC into a second year of operating in desert environments. In addition to this, laboratory work will continue on the SSC conductor taken from the field trial rig after 12months. With a study into organic contaminants on the surface using X-ray photoelectron spectroscopy (XPS). The effect of improved hydrophilicity and surface roughness changes on corona losses will be explored and finally the effect coated conductors have on impedance of transmission lines to understand if any protection changes will be needed.

Conclusion

This paper reports the results of a 12month field trial of a conductor with an SSC compared to an uncoated conductor. Peak cooling of 33.6% was demonstrated with an average cooling of ~6.3% across the year. The consistently high wind speeds at Al Fadhili, averaging ~4m/s, contributed to the large difference between peak and average cooling, with.

A side by side performance comparison of a brand new SSC coated conductor compared to those that have been in the field for 12months was presented and found no measurable thermal performance difference between them after the first 30days of

data (Δ~0.1°C). In addition to this thermal current cycling showed [enter]. Further, SEM confirmed that there was no significant reduction in film thickness relative to a new coated sample after 12 month samples. Finally, FTIR spectroscopy confirms there has been no change in the absorption of chemical bonds critical to material function, i.e. there has been no significant bond degradation. Hence, through systematic performance testing of aged and new samples, coupled with lab spectroscopy, we conclude the material is suitable for use in GCC environments.

Finally, laboratory data illustrated a significant improvement in hydrophilicity the SSC after 12months, suggesting a possible application for reducing corona losses [16].

References

[1] A. Al-Badi and I. AlMubarak, “Growing energy demand in the GCC countries,” *Arab J. Basic Appl. Sci.*, vol. 26, no. 1, pp. 488–496, 2019.

[2] O. Higbee, N. Coogan, A. Al-Thagafi "A Field Analysis of New Overhead Line Conductor Coatings to Increase Ampacity/Reduce Power Losses in Desert Environment: Performance and Durability Assessments" GCC Power 2021

[3] T. B. Cigré, “601,” *Guid. Therm. Rat. Calc. Overhead Lines, Work. Gr. B*, vol. 2, p. 43, 2014.

[4] ANSI C119, "Electric Connectors - Testing Methods and Equipment Common to the ANSI C119 Family of Standards"

[5] M. Bertinat, R. Wood, and E. Marquand, “Improved Statistical Ratings For Distribution Overhead Lines (Phase 2) Final Report,” 2018.

[6] Andrew Mills, James Hepburn, David Hazafy et al "A simple, inexpensive method for the rapid testing of the photocatalytic activity of self-cleaning surfaces", Journal of Photochemistry and Photobiology A: Chemistry, Volume 272, 2013, Pages 18-20.

[7] O. Armstrong, G. Southern, A. Carroll, and G. O’Brien, “Low wind speed occurrences and aging conductors: More than just a sag problem?,” in 2018 IEEE/PES Transmission and Distribution Conference and Exposition (T&D), 2018, pp. 1–5.

[8] "IEEE Guide for Cleaning Insulators," in IEEE Std 957-1995 , vol., no., pp.1-64, 23 Aug. 1995.

[9] Shadfan, H., Mashhady, A., Eter, A. and Hussen, A.A. (1984), "Mineral Composition of Selected Soils in Saudi Arabia." Z. Pflanzenernaehr. Bodenk., 147: 657-668.

[10] Lee, S.Y., Dixon, J.B. and Aba-Husayn, M.M. (1983), "Mineralogy of Saudi Arabian Soils: Eastern Region." Soil Science Society of America Journal, 47: 321-326.

[11] Koralegedara NH, Pinto PX, Dionysiou DD, Al-Abed SR. "Recent advances in flue gas desulfurization gypsum processes and applications - A review." J Environ Manage. 2019 Dec 1;251:109572.

[12] Qingxin Ma, Hong He, Yongchun Liu, Chang Liu and Vicki H. Grassian, Phys. Chem. Chem. Phys., 2013,15, 19196-19204

[13] Mohammed Benaafi, Osman Abdullatif, Arabian Journal of Geosciences, 2015, 8, 12, 11073-11092

[14] Bharti VK, Giri A, Kumar K (2017) "Fluoride Sources, Toxicity and Its Amelioration: A Review." Ann Environ Sci Toxicol 2(1): 021-032.

[15] X. M. Bian, L. Chen, D. M. Yu, L. M. Wang, and Z. C. Guan , "Surface roughness effects on the corona discharge intensity of long-term operating conductors", Appl. Phys. Lett. 101, 174103 (2012)

[16] J. Kim and M. K. Chaudhury, "Corona-discharge-induced hydrophobicity loss and recovery of silicones," 1999 Annual Report Conference on Electrical Insulation and Dielectric Phenomena (Cat. No.99CH36319), 1999, pp. 703-706 vol.2.